

*Microlensing 2000: A New Era of Microlensing Astrophysics*  
*ASP Conference Series, Vol. 000, 2000*  
*J.W. Menzies and P.D. Sackett, eds.*

## Microlensing Constraints on the Frequency of Jupiter Mass Planets

B. Scott Gaudi<sup>1</sup>, M.D. Albrow<sup>2</sup>, Jin H. An<sup>1</sup>, J.-P. Beaulieu<sup>3</sup>, J.A.R. Caldwell<sup>4</sup>, D.L. Depoy<sup>1</sup>, M. Dominik<sup>5</sup>, A. Gould<sup>1</sup>, J. Greenhill<sup>6</sup>, K. Hill<sup>6</sup>, S. Kane<sup>6</sup>, R. Martin<sup>7</sup>, J. Menzies<sup>4</sup>, R.W. Pogge<sup>1</sup>, K. Pollard<sup>8</sup>, P.D. Sackett<sup>5</sup>, K.C. Sahu<sup>2</sup>, P. Vermaak<sup>4</sup>, R. Watson<sup>6</sup>, A. Williams<sup>7</sup>  
 (The PLANET collaboration)

<sup>1</sup> *The Ohio State University*

<sup>2</sup> *Space Telescope Science Institute*

<sup>3</sup> *Institut d'Astrophysique de Paris*

<sup>4</sup> *South African Astronomical Observatory*

<sup>5</sup> *Kapteyn Astronomical Institute*

<sup>6</sup> *University of Tasmania*

<sup>7</sup> *Perth Observatory*

<sup>8</sup> *University of Canterbury*

**Abstract.** Microlensing is the only technique likely, within the next 5 years, to constrain the frequency of Jupiter-analogs. The PLANET collaboration has monitored nearly 100 microlensing events of which more than 20 have sensitivity to the perturbations that would be caused by a Jovian-mass companion to the primary lens. No clear signatures of such planets have been detected. These null results indicate that Jupiter mass planets with separations of 1.5-3 AU occur in less than 1/3 of systems. A similar limit applies to planets of 3 Jupiter masses between 1-4 AU.

## 1. Introduction

A Galactic microlensing event occurs when a massive, compact object (the lens) passes near to our line-of-sight to a more distant star (the source). If the lens, observer, and source are perfectly aligned, then the lens images the source into a ring, called the Einstein ring, which has angular radius of<sup>1</sup>

$$\theta_E \equiv \left[ \frac{4GM}{c^2} \frac{D_{LS}}{D_L D_S} \right]^{1/2} \sim 480 \mu\text{as} \left( \frac{M}{M_\odot} \right)^{1/2}, \quad (1)$$

---

<sup>1</sup>For the scaling relation on the far right of equations (1), (2), and (3), we have assumed  $D_S = 8$  kpc and  $D_L = 6.5$  kpc, typical distances to the lens and source for microlensing events toward the bulge.

where  $M$  is the mass of the lens, and  $D_{\text{LS}}$ ,  $D_{\text{S}}$ ,  $D_{\text{L}}$  are the lens-source, observer-source, and observer-lens distances, respectively. This corresponds to a physical distance at the lens plane of

$$r_{\text{E}} = \theta_{\text{E}} D_{\text{L}} \sim 3 \text{ AU} \left( \frac{M}{M_{\odot}} \right)^{1/2}. \quad (2)$$

If the lens is not perfectly aligned with the line-of-sight, then the lens splits the source into two images. The separation of these images is  $\mathcal{O}(\theta_{\text{E}})$  and hence unresolvable. However, the source is also magnified by the lens, by an amount that depends on the angular separation between the lens and source in units of  $\theta_{\text{E}}$ . Since the lens, observer, and source are all in relative motion, this magnification is a function of time: a ‘microlensing event.’ The time scale for such an event is

$$t_{\text{E}} \equiv \frac{\theta_{\text{E}}}{\mu_{\text{rel}}} \sim 40 \text{ days} \left( \frac{M}{M_{\odot}} \right)^{1/2}, \quad (3)$$

where  $\mu_{\text{rel}}$  is the relative lens-source proper motion.

If the primary lens has a planetary companion, and the position of this companion happens to be in the path of one of the two images created during the primary event, then the planet will perturb the light from this image, creating a deviation from the primary light curve (see Figure 1). The duration of this perturbation is  $\sim \sqrt{q} t_{\text{E}}$ , where  $q$  is the mass ratio between the planet and primary. Hence, for a Jupiter/Sun mass ratio ( $q \simeq 10^{-3}$ ), the perturbation time scale is  $\mathcal{O}(\text{day})$ . These short-duration deviations are the signatures of planets orbiting the primary lenses. Note that since the perturbation time scale is considerably less than  $t_{\text{E}}$ , the majority of the light curve will be indistinguishable from a single lens.

Three parameters determine the magnitude of the perturbation, and hence define the observables. These are mass ratio  $q$ , the instantaneous angular separation  $d$  between the planet and primary in units of  $r_{\text{E}}$ , and the angle  $\alpha$  between the projected planet/star axis and the path of the source. As  $q$  decreases, the perturbation time scale decreases, although the magnitude of the deviation does not necessarily decrease. Thus very small mass ratio planets ( $q \lesssim 10^{-5}$ ) can be detected using microlensing, although the detection probability is small. The lower limit to the detectable  $q$  is set practically by the sampling of the primary event, and ultimately by the finite size of the source stars (Bennett & Rhie 1996). A microlensing event is generally alerted only if the minimum angular impact parameter in units of  $\theta_{\text{E}}$  satisfies  $u_0 \leq 1$ , which corresponds to image positions between  $(0.6 - 1.6)\theta_{\text{E}}$ . Since the planet must be near one of these images to create a perturbation, microlensing is most sensitive to planets with separations  $0.6 \lesssim d \lesssim 1.6$ , the ‘lensing zone.’ The angle  $\alpha$ , which is of no physical interest, is uniformly distributed. Only certain values of  $\alpha$  will create detectable deviations. Thus integration over  $\alpha$  defines a geometric detection probability.

Microlensing as a method to detect extrasolar planets was first suggested by Mao & Paczyński (1991), and was expanded upon by Gould & Loeb (1992) who demonstrated that if all lenses had a Jupiter analog, then  $\sim 20\%$  of all light curves should exhibit  $\gtrsim 5\%$  deviations. Since these two seminal papers, many authors have explored the use of microlensing to detect planets. It is

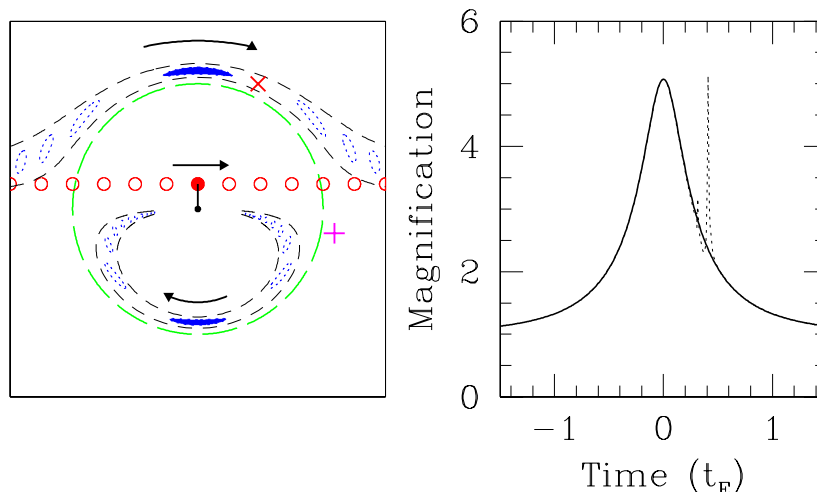


Figure 1. Left: The images (dotted ovals) are shown for several different positions of the source (solid circles), along with the primary lens (dot) and Einstein ring (long dashed circle). If the primary lens has a planet near the path of one of the images, i.e. within the short-dashed lines, then the planet will perturb the light from the source, creating a deviation to the single lens light curve. Right: The magnification as a function of time is shown for the case of a single lens (solid) and accompanying planet (dotted) located at the position of the X in the top panel. If the planet was located at the + instead, then there would be no detectable perturbation, and the resulting light curve would be identical to the solid curve.

not our intention to provide a comprehensive review of this field. However, of particular relevance is the paper by Griest & Safizadeh (1998, GS98) who demonstrated that, for high-magnification events (those with maximum magnification  $A_{\max} > 10$ ), the detection probability for planets in the lensing zone is  $\sim 100\%$ . Thus high-magnification events are an extremely efficient means of detecting extrasolar planets. The results of GS98 also imply that multiple planets in the lensing zone should betray their presence in high-magnification events (Gaudi, Naber & Sackett 1998).

## 2. Limits on Companions in OGLE-1998-BUL-14

The basic requirements to detect planets with microlensing are good temporal sampling and photometric precision. Since the optical depth to microlensing is low,  $\mathcal{O}(10^{-6})$ , the survey teams that discover microlensing events toward the Galactic bulge must monitor of order one million stars on a nightly basis in order to detect any events. Therefore, they generally have insufficient sampling to detect the short-duration perturbations to the primary light curve (see, e.g., Figure 2). However, these survey teams (OGLE, Udalski et al. 1994; MACHO, Alcock et al. 1996; EROS; Glicenstein et al., these proceedings) issue alerts, notification

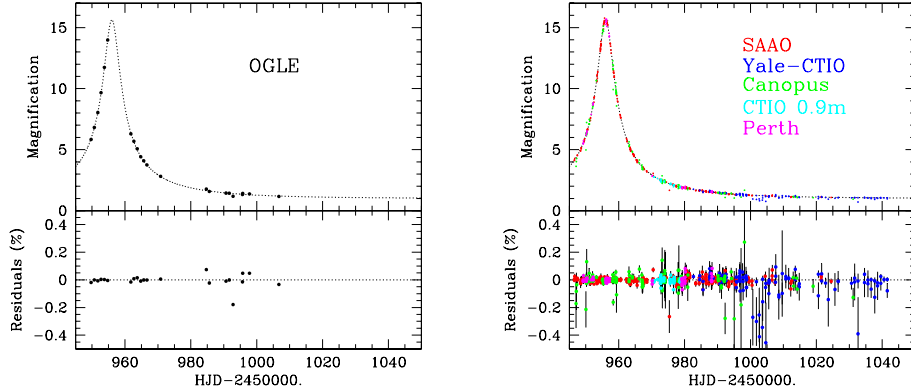


Figure 2. Left: The top panel shows the magnification as a function of time for OGLE data of microlensing event OGLE-1998-BUL-14. The dashed line indicates the best-fit point-source point-lens model (PSPL), which has a time scale  $t_E = 40$  days, and a maximum magnification of  $\sim 16$ . The bottom panel shows the residuals from the best-fit PSPL model. Right: The top panel shows the magnification as a function of time for PLANET data of microlensing event OGLE-1998-BUL-14. The bottom panel shows the residuals from the best-fit PSPL model (Albrow et al. 2000).

of ongoing events. This allows follow-up collaborations (GMAN, Alcock et al. 1997; PLANET, Albrow et al. 1998; MPS, Rhie et al. 1999; MOA, Yock, these proceedings) to monitor these events frequently with high-quality photometry to search for planetary deviations. In particular, the PLANET collaboration has access to four telescopes located in Chile, South Africa, Western Australia, and Tasmania, and can monitor events nearly round-the-clock, weather permitting.

Figure 2 shows PLANET photometry of an event alerted by the OGLE collaboration, OGLE-1998-BUL-14. This was a high-magnification event ( $A_{\max} \sim 16$ ) with  $t_E \simeq 40$  days, making it an excellent candidate to search for planetary deviations. PLANET obtained a total of 600 data points for this event: 461  $I$ -band and 139  $V$ -band. The median sampling interval is about 1 hour, or  $10^{-3}t_E$ , with very few gaps greater than 1 day. The  $1\sigma$  scatter in  $I$  over the peak of the event (where the sensitivity to planets is the highest) is 1.5%. The dense sampling and excellent photometry means that our efficiency to detect massive companions should be quite high. In fact, examination of the residuals from a single lens model (Fig. 2) reveal no obvious deviations of any kind.

To be more quantitative, we simultaneously search for binary-lens fits and calculate the detection efficiency  $\epsilon(d, q)$  of OGLE-1998-BUL-14 as a function of separation and mass ratio using a method proposed by Gaudi & Sackett (2000). For details on the implementation for this event, see Albrow et al. (2000).

We find no binary-lens models in the parameter ranges  $0 \leq d \leq 4$  and  $10^{-5} \leq q \leq 1$  that provide significantly ( $\Delta\chi^2 \gtrsim 10$ ) better fits to the OGLE-

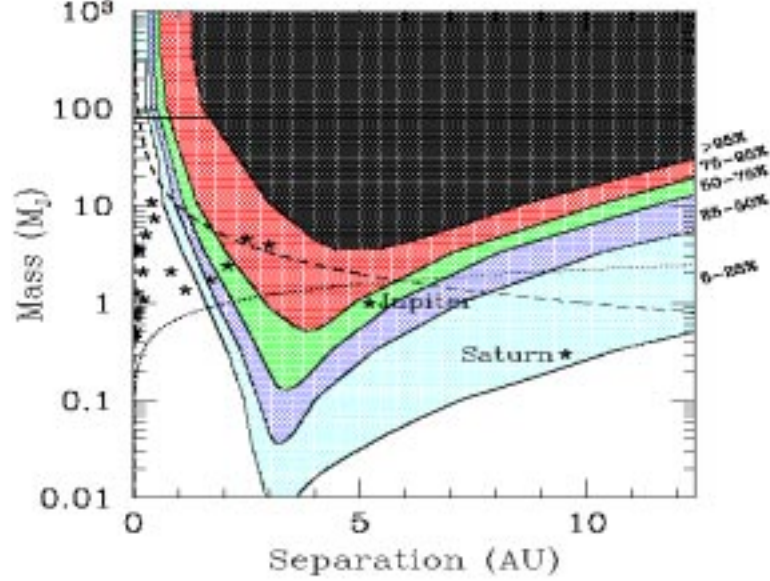


Figure 3. Detection efficiencies for the PLANET data set of OGLE-1998-BUL-14 as a function of the mass and orbital separation of the companion assuming a primary lens mass of  $M_{\odot}$  and Einstein ring radius of  $r_E = 3.1$  AU. The contours are (outer to inner) 5%, 25%, 50%, 75% and 95%. In order to convert from mass ratio and projected separation to mass and physical separation, we have averaged over orbital phase and inclination (assuming circular orbits). Jupiter and Saturn are marked with stars, as are the extrasolar planets discovered with radial velocity techniques. The horizontal line marks the hydrogen-burning limit. The dotted line shows the radial-velocity detection limit for an accuracy of  $20 \text{ ms}^{-1}$  and a primary mass of  $M_{\odot}$ . The dashed line is the astrometric detection limit for an accuracy of 1 mas and a primary of mass  $M_{\odot}$  at 10 pc (Albrow et al. 2000).

1998-BUL-14 dataset. We therefore conclude that the light curve of OGLE-1998-BUL-14 is consistent with a single lens.

In Figure 4 we show the detection efficiency  $\epsilon$  of our OGLE-1998-BUL-14 dataset to companions as a function of the mass  $M_p$  and orbital radius  $a$  of the companion. Parameter combinations shaded in black are excluded at the 95% significance level. Stellar companions to the primary lens of OGLE-1998-BUL-14 with separations between  $\sim 2$  AU and 11 AU are excluded. Companions with mass  $\geq 10 M_J$  are excluded between 3 AU and 7 AU. Although we cannot exclude a Jupiter-mass companion at any separation, we had a  $\sim 80\%$  chance of detecting such a companion at 3 AU. The detection efficiency for OGLE-1998-BUL-14 is  $> 25\%$  at  $a = 3$  AU for all companion masses  $M_p > 0.03 M_J$ . We find that we had a  $\sim 60\%$  chance of detecting a companion with the mass and separation of Jupiter ( $M_p = M_J$  and  $a = 5.2$  AU), and a  $\sim 5\%$  chance of

detecting a companion with the mass and separation of Saturn ( $M_p = 0.3 M_J$  and  $a = 9.5$  AU) in the light curve of OGLE-1998-BUL-14.

Thus, although Jupiter analogs cannot be ruled out in OGLE-1998-BUL-14, the detection efficiencies are high enough that non-detections in several events with similar quality will be sufficient to place meaningful constraints on their abundance.

How do the OGLE-1998-BUL-14 efficiencies compare to planet detection via other methods? In Figure 4 we show the radial velocity detection limit on  $M_p \sin i$  for a solar mass primary as a function of the semi-major axis for a velocity amplitude of  $K = 20 \text{ m s}^{-1}$ , which is the limit found for the majority of the stars in the Lick Planet Search (Cumming, Marcy & Butler 1999). Although we show this limit for the full range of  $a$ , in reality the detection sensitivity extends only to  $a \lesssim 5$  AU due to the finite duration of radial-velocity planet searches and the fact that one needs to observe a significant fraction of an orbital period. In addition, we plot in Figure 4 the  $M_p \sin i$  and  $a$  for planetary candidates detected in the Lick survey. Radial velocity searches clearly probe a different region of parameter space than microlensing, in particular, smaller separations. Note, however, that our OGLE-1998-BUL-14 data set gives us a  $> 75\%$  chance of detecting analogs to two of these extrasolar planets: the third companion to Upsilon And and the companion to 14 Her. Although the efficiency is low, we do have sensitivity to planets with masses as small as  $\sim 0.01 M_J$ , considerably smaller than can be detected via radial velocity methods. For comparison, we also show in Figure 10 the astrometric detection limit on  $M_p$  for a  $M_\odot$  primary at 10 pc, for an astrometric accuracy of  $\sigma_A = 1$  mas. For an astrometric campaign of 11 years, this limit extends to  $\sim 5$  AU. Such an astrometric campaign ( $\sigma_A = 1$  mas,  $P = 11$  years), would be sensitive to companions similar to those excluded in our analysis of OGLE-1998-BUL-14. The proposed Space Interferometry Mission (SIM) promises  $\sim 4 \mu\text{as}$  astrometric accuracy, which would permit the detection of considerably smaller mass companions.

### 3. Combined Limits from the 1998-1999 PLANET Seasons

Clearly one cannot make any statements about the population of the extrasolar planets as a whole based on one event. Fortunately, PLANET has monitored, over the last five years, more than 100 events, a subset of which have temporal sampling and photometric accuracy similar to that of OGLE-1998-BUL-14. Here we present a preliminary analysis of these events.

We select 23 high-quality light curves from the 1998-1999 PLANET seasons and analyze these in the same manner as OGLE-1998-BUL-14 (Albrow et al. 2000). Included in this sample are 5 high-magnification ( $A_{\text{max}} > 10$ ) events: OGLE-1998-BUL-14, MACHO-1998-BUL-35, OGLE-1999-BLG-5, OGLE-1999-BUL-35 and OGLE-1999-BUL-36.

We find that all 23 events are consistent with a single lens to within our detection threshold. Using this null result, along with the detection efficiency  $\epsilon_i(d, q)$  for each event  $i$ , we find a statistical upper limit to the fraction of these lenses that have a companion of a given separation and mass ratio. If the fraction of lenses with a companion as a function of  $d$  and  $q$  is  $f(d, q)$ , then probability that  $N$  events with individual efficiencies  $\epsilon_i(d, q)$  would give a null result (no

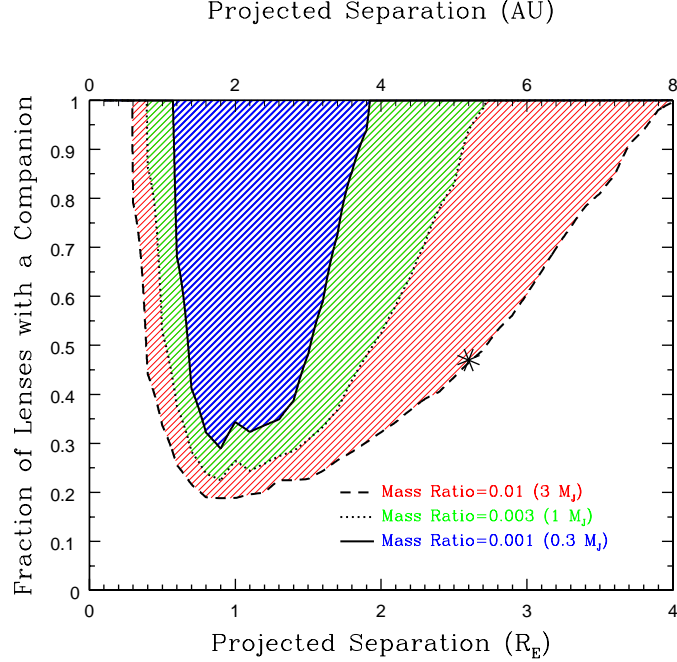


Figure 4. Upper limits to the fraction of primary lenses with a companion as a function of the projected separation in  $r_E$  for three different mass ratios,  $q = 10^{-2}$  (dashed),  $q = 10^{-2.5}$  (dotted) and  $q = 10^{-3.0}$  (solid). The projected separation in AU assuming all primary lenses are at 6 kpc and have masses of  $0.3 M_\odot$  is shown in the top axis. Similarly, masses of the secondary are shown in parentheses. These upper limits are at the 95% confidence level and are based on 23 events.

detections) is,

$$P = \prod_{i=1}^N [1 - f(d, q) \epsilon_i(d, q)]. \quad (4)$$

The 95% confidence level (c.l.) upper limit to  $f(d, q)$  is found by setting  $P = 5\%$ .

In Figure 4 we show the 95% c.l. upper limits to  $f(d, q)$  for separations  $0 \leq d \leq 4$  and  $q = 10^{-2}, 10^{-2.5}$ , and  $10^{-3}$ . We convert these to limits on the fraction of lenses with companions of a given mass and physical separation by assuming that all the primaries have mass  $M = M_\odot$  and distance  $D_L = 6$  kpc. We find that  $< 33\%$  of these lenses have Jupiter mass planets with separations of 1.5-3 AU. Similarly,  $< 33\%$  have planets of mass  $M_p \geq 3 M_J$  with separations of 1-4 AU. Although we cannot place an interesting limit on Jupiter analogs, we do find that  $< 50\%$  of lenses have  $3 M_J$  planets at the separation of Jupiter (5.2AU).

#### 4. Conclusions

Microlensing offers a unique and complementary method of detecting extrasolar planets. Although many light curves have been monitored in the hopes of detecting the short-duration signature of planetary companions to the primary lenses, no convincing planetary detections have yet been made, despite the fact that data of sufficient quality are being acquired to detect such companions. These null results indicate that Jupiter-mass companions with separations in the ‘lensing zone,’  $1.5 - 3$  AU, occur in less than  $1/3$  of systems.

The potential for this field is enormous. Current microlensing searches for planets will continue to monitor events alerted toward the bulge, and either push these limits down to levels probed by radial velocity surveys ( $\sim 5\%$ ), or finally detect planets, and measure the frequency of companions at separations more relevant to our solar system. Next generation microlensing planet searches have the promise of obtaining a robust statistical estimate of the fraction of stars with planets of mass as low as that of the Earth.

**Acknowledgments.** We thank the MACHO, OGLE and EROS collaborations for providing real-time alerts. We are especially grateful to the observatories that support our science (Canopus, CTIO, Perth and SAAO) via the generous allocations of time that make this work possible. This work was supported by grants AST 97-27520 and AST 95-30619 from the NSF, by grant NAG5-7589 from NASA, by a grant from the Dutch ASTRON foundation through ASTRON 781.76.018, by a Marie Curie Fellowship from the European Union, by “coup de pouce 1999” award from Ministère de l’Éducation nationale, de la Recherche et de la Technologie, and by a Presidential Fellowship from the Ohio State University.

#### References

- Albrow, M., et al. 1998, *ApJ*, 509, 687
- Albrow, M., et al. 2000, 535, 000 (astro-ph/9909325)
- Alcock, C., et al. 1996, *ApJ*, 463, L67
- Alcock, C., et al. 1997, *ApJ*, 491, 436
- Bennett, D. & Rhie, S. H. 1996, *ApJ*, 472, 660
- Cumming, A., Marcy, G., & Butler, R.P. 1999, *ApJ*, 526, 890
- Gaudi, B. S., Naber, R. M., & Sackett, P. D. 1998, *ApJ*, 502, L33
- Gaudi, B. S., & Sackett, P. D. 2000, *ApJ*, 529, 56
- Gould, A., & Loeb, A. 1992, *ApJ*, 396, 104
- Griest, K., & Safizadeh, N. 1998, *ApJ*, 500, 37
- Mao, S., & Paczyński, B. 1991, *ApJ*, 374, 37
- Rhie, S.H., et al. 1999, *ApJ*, 522, 1037
- Udalski, A., et al. 1994, *Acta Astron.*, 44, 227